

Influence of Ageing time and Stress on Corrosion behavior of AA2024-T6 in saturated NaCl Solution

Zaigham Saeed Toor, Ishaq Ahmed, Sajid Ullah, Akbar Niaz Butt, Syed Wilayat Hussain

Abstract— Effect due to ageing time and stress on the corrosion behavior of Aluminum-Copper alloy AA 2024-T6 is studied. The alloy specimens were aged for 6 hrs, 9 hrs and 12 hrs ageing time and then subjected to corrosion testing in saturated Sodium Chloride (NaCl) solution. Constant Stress of 0.25 δ_y (yield strength) using four point bend apparatus is applied on a 9 hrs aged sample and this setup is immersed in the saturated NaCl solution to study the effect of stress. Polarization curves of the aged specimens having same exposed area showed that the specimens corroded majorly by pitting mechanism which is supported from SEM micrographs. The sample aged for 9 hrs had the least corrosion resistance but the samples aged for 6 hrs and 12 hrs had 11% and 28% increase in the corrosion resistance. However, the sample aged for 9 hrs had the highest hardness, making it a good candidate out of the three for structural applications where corrosion resistance is also important. Polarization curves of non-stressed and stressed specimens having same exposed area showed a 70% increase in the corrosion rate of the latter, calculated from the marked area of the polarization curves along with a decrease in the passive region. The former corroded by pitting mechanism while the latter corroded by film-dissolution mechanism which is inferred from SEM micrographs.

Index Terms— Aerospace materials, Corrosion, Electrode Kinetic Measurements, Stress Corrosion Cracking

I. INTRODUCTION

Aluminum and its alloys are extensively used in the field of Aerospace due to their high specific strength. The significance of these heat treatable alloys can be analyzed from the fact that their strength can be increased up to 17 times than their original strength values using ageing treatment at an affordable cost [1-3]. However the major setback of these treatments is the reduction in the corrosion resistance with the sequential increase in strength [4]. More detrimental effects of corrosion are observed when these alloys are used in stress based applications, termed as stress corrosion cracking [5].

For the purpose of evaluation of these phenomenon, which are localized in nature, Electrode Kinetic Measurements (EKM) can be performed to investigate and understand their

corrosion behavior [6, 7]. Precipitation hardening or age hardening is a heat treatment process for strengthening heat treatable alloys by precipitate growth. By over aging the samples, which will coarsen the precipitates, present in the matrix, we can improve corrosion behavior. This could be attributed to the less number of micro-galvanic cells formed between the matrix and the precipitates. However, the strength of the alloy is reduced due to coarser structure [1].

In this study, the corrosion behavior for AA 2024-T6 artificially aged for 6 hrs, 9 hrs and 12 hrs and the effect of applied tensile stress for artificially aged for 9 hrs specimens in saturated NaCl solution is studied using GAMRY potentiostat and corrosion resistance of both stressed and non-stressed specimens is calculated from potentiodynamic polarization curves.

II. EXPERIMENTAL PROCEDURE

In order to study the effect of ageing time on corrosion behavior of AA2024-T6 in saturated NaCl Solution, cube (10 mm x 10 mm x 2 mm) specimens of AA2024-T6, artificially aged at 190°C for 6 hrs, 9 hrs and 12hrs after solution treatment at 495°C and to study the effect of stress on corrosion behavior of AA2024-T6 in saturated NaCl Solution, Sheet (130 mm x 30 mm x 2 mm) specimens of AA2024-T6, artificially aged at 190°C for 9 hrs after solution treatment at 495°C, were provided by Institute of Space Technology (IST), Islamabad, Pakistan. Fig. 1 to Fig. 3 exhibits the Temperature Time Transformation (TTT) diagram, ageing time versus hardness and the stress-strain curve of the alloy used in the study from available literature for design and comparison [8-10]. The chemical composition done by SEM-Energy Dispersive X-ray Spectroscopy (EDS), temper designation and hardness (Vickers hardness tester at 10 kgf) are shown in Table I. The alloy was tested in saturated NaCl at room temperature (25°C).

Specimen preparation was done before starting the test in accordance with American Society for Testing and Materials (ASTM) standards G-39, G-5 and relevant literature [11-14]. The samples were subjected to mechanical grinding using Silicon Carbide (SiC) emery paper ranging from 350 grit to 2000 grit size, followed by Alumina paste (1 μ m particle size) polishing. The specimens were washed on intervals with distilled water during the grinding and polishing operation and

Manuscript received March 21, 2018.

Engr. Zaigham Saeed Toor is a graduate of Materials Science & Engineering Department, Institute of Space Technology (IST), Islamabad, Pakistan. He is a registered engineer with Pakistan Engineering Council (PEC) (email: zaighamtoor93@gmail.com)

also after the preparation was completed. An exposed area of 2.5cm² was maintained in the cube (non-stressed) and sheet (stressed) specimen after insulation and stress application respectively. The non-stressed specimen was embedded with epoxy resin except the exposed area as shown in Fig. 4. Four point bend apparatus [11] was connected with the Potentiostat for electrode kinetic measurements to study the corrosion behavior of sheet specimen under applied stress. The sheet specimen was electrically connected with potentiostat by soldering the single strand copper wire to the specimen surface, covering and insulating the entire specimen with epoxy except the central, most stressed region of the specimen as shown in Fig. 4. The sheet specimen was mounted in the apparatus and a tensile stress of 80 MPa (0.25 δ_y) was applied [11].

Electrochemical measurements in terms of potentiodynamic polarization tests were conducted at room temperature (25°C), in stagnant saturated NaCl solution (pH 7.0 at 25°C) at a scanning rate of 1mV/s. A conventional three-electrode Pyrex cell comprising of saturated calomel electrode (SCE) as reference, was connected to the working solution using Luggin probe. Platinum network was used as auxiliary electrode [13, 14]. The testing was performed using ©GAMRY Instruments, Inc. potentiostat and the output current was recorded using Gamry Framework module connected to a personal computer for in-situ potentiodynamic polarization curves. The anodic and cathodic polarization curves were analyzed using Gamry Echem Analyst, Version 6.10 module to determine corrosion rates in mils per year (mpy) as shown in Table II.

Scanning Electron Microscopy (SEM) of the tested specimens was done using MIRA3 TESCAN SEM InBeam and Secondary Electron (SE) modes. SEM-Energy Dispersive X-ray Spectroscopy (EDS) was done for compositional analysis of the received alloy and corrosion product as shown in Table I and Table III respectively.

TABLE I

Chemical analysis and Hardness of Aluminum alloy used in this study			
Alloy AA	2024	2024	2024
Si	0.16	0.16	0.16
Fe	0.5	0.5	0.5
Cu	4.56	4.56	4.56
Mn	0.46	0.46	0.46
Mg	1.33	1.33	1.33
Cr	0.0004	0.0004	0.0004
Zn	0.0013	0.0013	0.0013
Ti	0.017	0.017	0.017
Al	Balance	Balance	Balance
Temper	T-6	T-6	T-6
Designations	(6hrs aged)	(9hrs aged)	(12hrs aged)
Hardness (VHN)	153	159	130

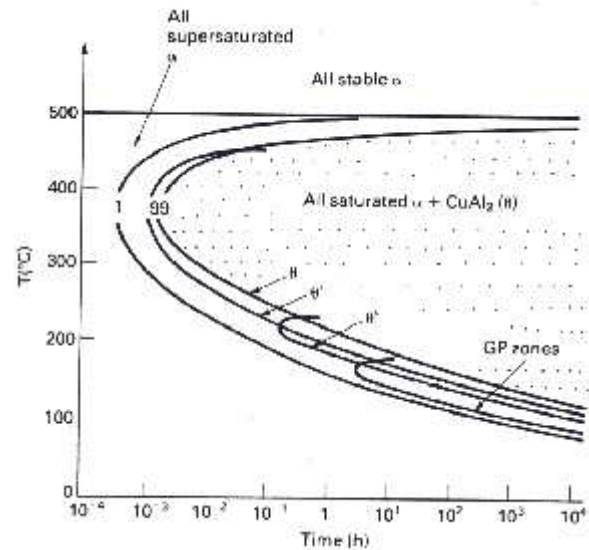


Fig. 1. TTT diagram of AA2024[10]

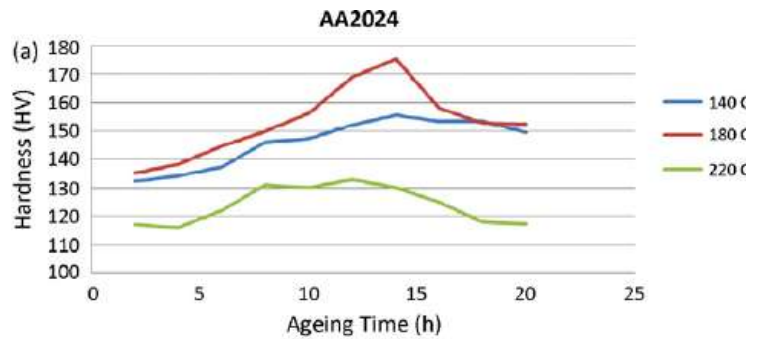


Fig. 2. Ageing time versus Hardness relation with reference to artificial ageing temperature[9]

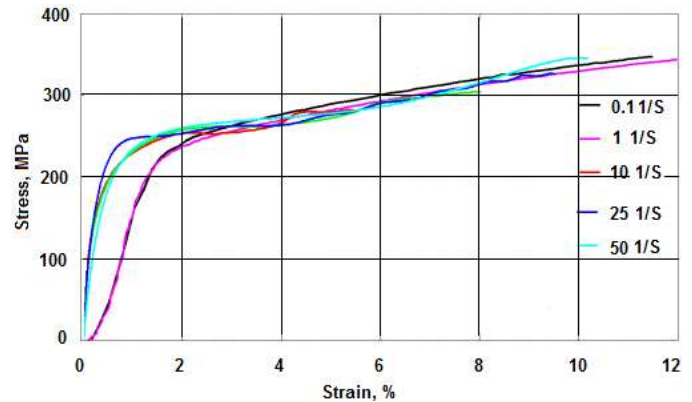


Fig. 3. Stress-Strain behavior of AA2024[8]



Fig. 4. Sheet specimen (a) Soldered and insulated with epoxy backside, (b) Front side exposing only the most stressed region, (c) mounted in Four point bend apparatus, (d) Four point bend apparatus mounted with specimen is connected with GAMRY Potentiostat for potentiodynamic test.



Fig. 5. Polished specimens of AA 2024-T6 insulated with epoxy except test surface for Potentiodynamic test.

III. RESULTS & DISCUSSION

Fig. 6 shows the polarization curves for AA2024-T6 (6 hrs, 9 hrs and 12 hrs) specimens in saturated NaCl solution at room temperature (25°C). The corrosion rates, free corrosion potential (E_{corr}) and pitting potential (E_{pit}) is also shown in Table II. It can be seen that a reasonable level of passivation is observed by the increase in anodic polarization escalating upwards till the pitting potential for the three specimens, above which the current density sharply increases. This can be attributed to the high positive potential applied that ruptures the passive oxide film at random weak points and cannot repair itself due to which localized corrosion develops at these points [7, 15] as shown in Fig. 6. On ionic scale, it can be explained by the excess of chloride (Cl^-) ions in the solution due to saturated NaCl. The excess chloride ions and the oxygen from air readily polarize the alloy to the pitting potential as discussed in literature [14, 15]. Thus irrespective of

the aging treatment, the specimens have corroded by pitting.

The polarization curves of the specimens also show that the sample aged for 9 hrs exhibits a decrease in the corrosion potential and an increase in the current density as compared to the sample aged for 6 hrs along with an increase in the corrosion rate by 11% as shown in Table II. This can be attributed to the formation of precipitates at 9 hrs ageing time, which results in formation of excess micro galvanic cells that provide more corrosion sites and hence increase the corrosion rates [1, 16]. The sample aged for 12 hrs exhibits an increase in the corrosion potential and a decrease in the current density as compared to the sample aged for 6 hrs along with a decrease in the corrosion rate by 19% as shown in Table II. This can be attributed to the precipitate coarsening effect at 12 hrs ageing time, which causes the reduction in number of micro galvanic cells that reduces the number of corrosion sites and hence decreases the corrosion rate [1, 16]. Fig. 7, Fig. 8 and Fig. 9, shows the SEM micrographs of the specimens exhibiting pitting at different resolutions [14]. It can be inferred that the SEM micrographs clearly supplement the polarization curves and literature indicated by the pits and mechanism discussed [8, 10, 11, 13].

Fig. 10 shows the polarization curves for AA2024-T6 (9 hrs) specimens in saturated NaCl solution at room temperature (25°C). The corrosion rates, free corrosion potential (E_{corr}) and pitting potential (E_{pit}) is also shown in Table II. It can be seen that for the non-stressed sample a reasonable level of passivation is observed by the increase in anodic polarization escalating upwards till the pitting potential, above which the current density sharply increases. This can be attributed to the high positive potential applied that ruptures the passive oxide film at random weak points and cannot repair itself due to which localized corrosion develops at these points [15] as shown in Fig. 4. On ionic scale, it can be explained by the excess of chloride (Cl^-) ions in the solution due to saturated NaCl. The excess chloride ions and the oxygen from air readily polarize the alloy to the pitting potential as discussed in literature [14, 15].

The polarization curve of the stressed specimen can be seen to have undergone prominent deviation from its counter-part. The corrosion potential has decreased and the current density has increased with the stress application which has increased the corrosion rate by 70% as shown in Table II [17]. It can be seen that as compared to its counter-part, passivation and prominent pitting potential is not observed in the curve. This can be attributed to the combined effect of stress and excess chloride ions in the solution that leads to passive film breakdown by film dissolution at a localized region [17]. This localized dissolution is coupled with a localized passive layer plastic deformation that prevents the reformation of the passive film in that region and thus ensures further localized dissolution. Cracking then proceeds by repeated cycles of deformation and dissolution [17, 18] as shown in Fig. 12.

Fig. 11 and Fig. 12 show the SEM micrographs of the non-stressed and stressed specimens respectively with the former

exhibiting pitting and the latter exhibiting film cracking and dissolution model [14, 15, 17, 18]. Fig. 13 shows the area selected for compositional analysis of the corrosion product layer using EDS and the corresponding compositions are shown in Table III, which confirms that the product layer is the passive Aluminum oxide (Al₂O₃), indicated by the high percentage of Aluminum and oxygen [5, 6, 14, 15, 17, 18].

TABLE II
Corrosion rates from polarization curves

Ageing time	6hrs	9hrs	12hrs	9hrs (Stressed)
β_a (V/decade)	1.53	1.47	1.59	0.453
β_c (V/decade)	0.115	0.129	0.108	0.714
I_{corr} (μA)	0.213	2.24	0.032	159
E_{corr} (mVsce)	-232	-964	703	-1332
E_{pit} (mVsce)	380	-587	1311	N.A
Corrosion rate (mpy)	0.856	0.962	0.692	3.586

Table III
Chemical analysis of the corrosion product

Element	Atomic %
O	74.52
Na	0.13
Al	22.04
Si	0.16
S	0.86
Cl	1.49
Ca	0.49
Zn	0.31

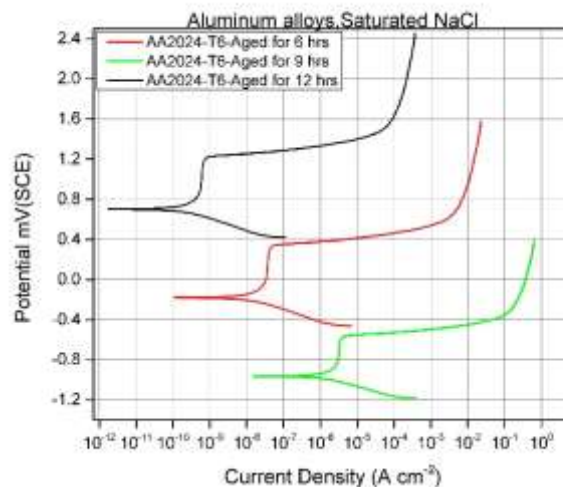


Fig. 6. Potentiodynamic polarization curves for Aluminum alloy (AA2024-T6) aged for 6 hrs, 9 hrs and 12 hrs tested in saturated NaCl solution at 25°C (scan rate is 1 mV/s).

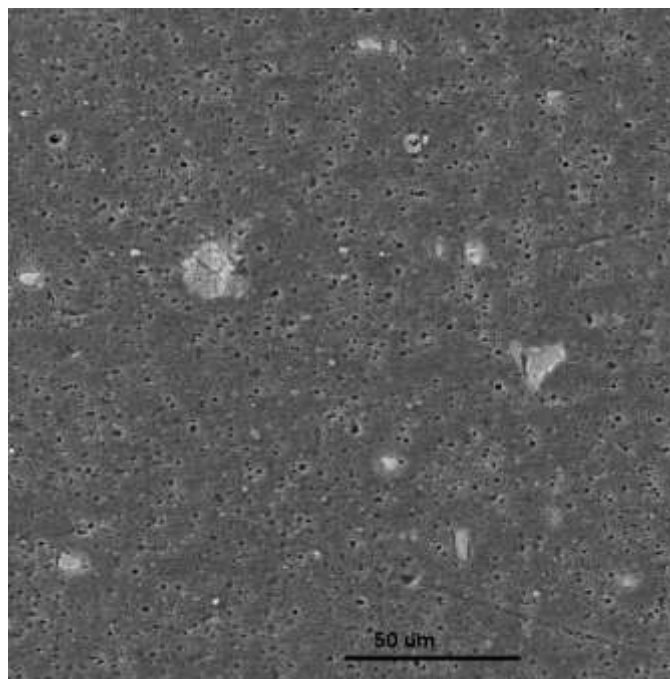


Fig. 7. SEM micrograph of AA2024-T6 exhibiting pitting after potentiodynamic test in saturated NaCl solution at 50 μm.

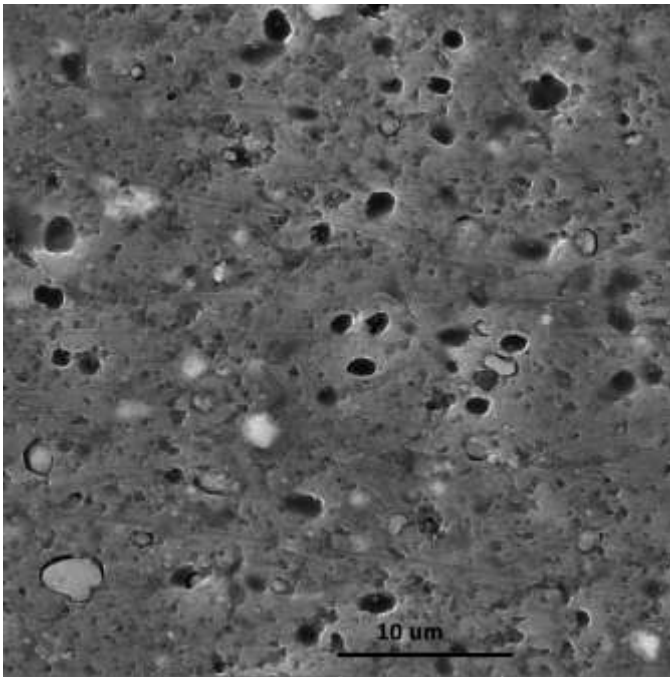


Fig. 8. SEM micrograph of AA2024-T6 exhibiting pitting after potentiodynamic test in saturated NaCl solution at 10 μm .

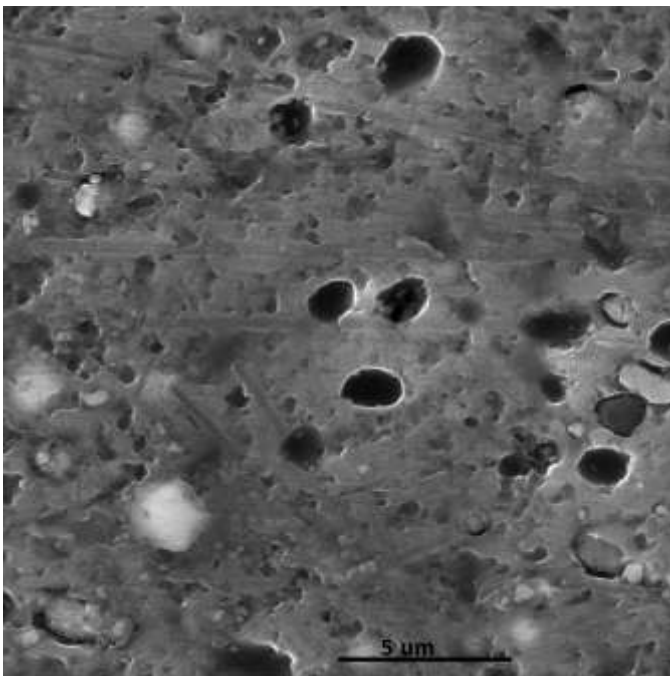


Fig. 9. SEM micrograph of AA2024-T6 exhibiting pitting after potentiodynamic test in saturated NaCl solution at 5 μm .

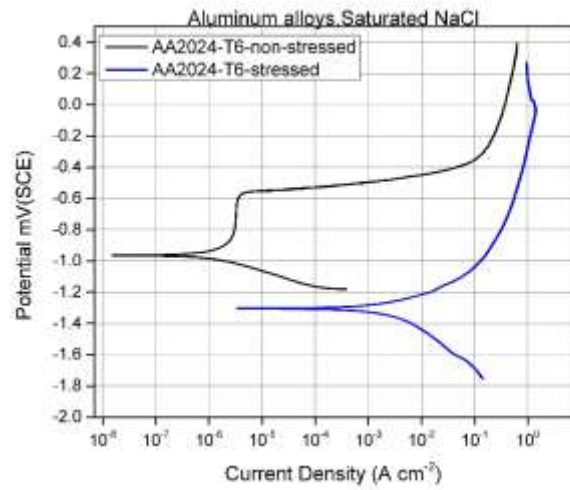


Fig. 10. Potentiodynamic polarization curves for Aluminum alloy (AA2024) in saturated NaCl solution at 25°C (scan rate is 1 mV/s).

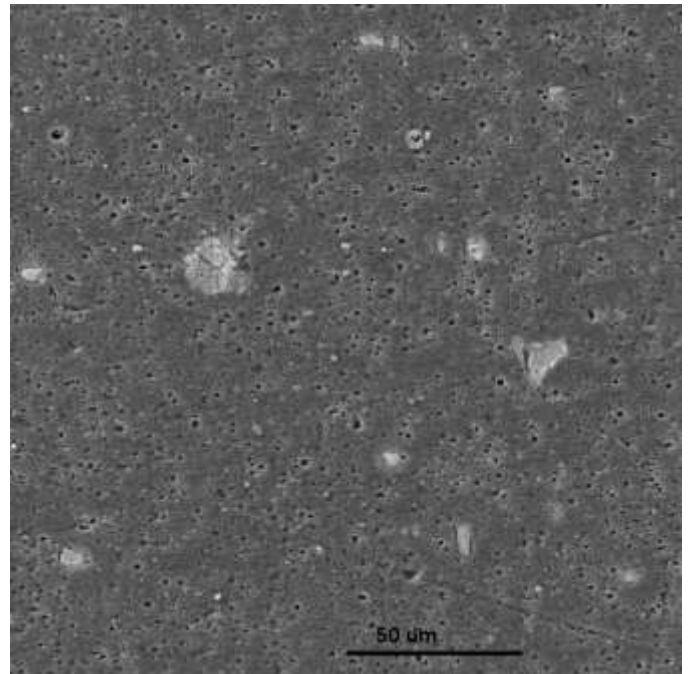


Fig. 11. SEM micrograph of AA2024-T6 exhibiting pitting after potentiodynamic test in saturated NaCl solution

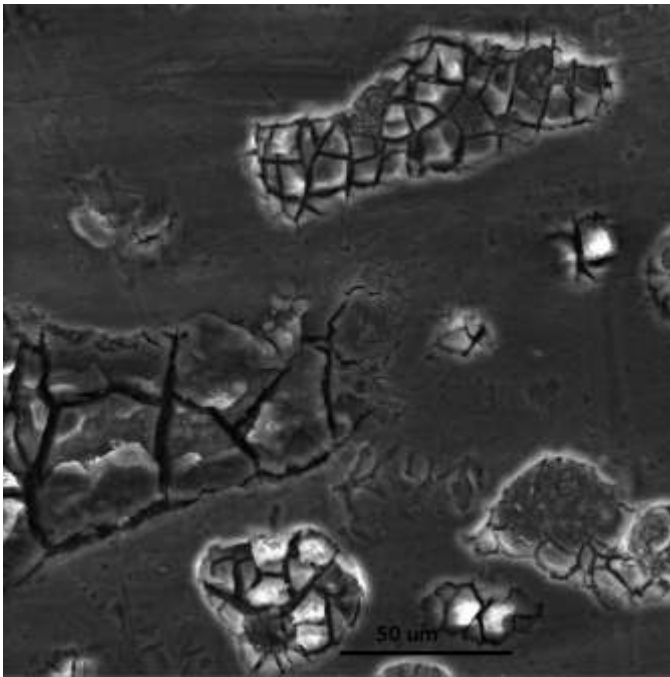


Fig. 12. SEM micrograph of AA2024-T6 exhibiting Layer breakage and dissolution phenomena in saturated NaCl solution due to stress application.

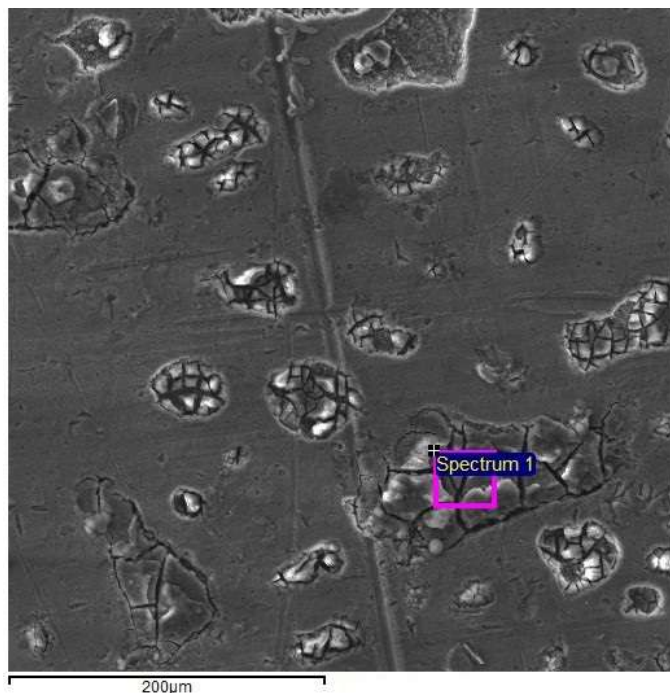


Fig. 13. SEM micrograph of AA2024-T6 exhibiting area selection for chemical analysis of corrosion product as highlighted by spectrum 1.

IV. CONCLUSION

- AA2024-T6 aged for 6 hrs, 9 hrs and 12 hrs corrodes by pitting mechanism in stagnant saturated NaCl solution at room temperature (25°C) with corrosion rates of 0.856, 0.962 and 0.692 mpy respectively.
- AA2024-T6 aged for 9 hrs exhibited the highest hardness, making it a good candidate out of the

three for structural applications where corrosion resistance is also important.

- The maximum decrease in corrosion rate was 28% for the sample aged for 12 hrs in comparison with the maximum corrosion rate observed at 9 hrs ageing time.
- AA2024-T6 (artificially aged for 9 hrs) corrodes by film-dissolution/rupture mechanism in stagnant saturated NaCl solution at room temperature (25°C) with an applied stress of 0.25δ, and exhibits a corrosion rate of 3.586 mpy, which is approximately 70% increase in corrosion rate as compared to its counterpart.
- The alloy having good corrosion resistance in a particular medium cannot be necessarily used for a Stress Corrosion Cracking (SCC) application in the same medium and a prior test of SCC is mandatory.
- Potentiodynamic corrosion testing for both metallurgical and medical based applications can be done using the testing setup which can have promising prospects in Oil & gas, Biomedical and Quality departments in terms of field and accelerated testing.

ACKNOWLEDGMENT

The authors would like to thank Dr. Syed Wilayat Hussain and Dr. Akbar Niaz Butt of Institute of Space Technology, who effectively supervised our research work. We appreciate the policies and support of Materials department at Institute of Space Technology for providing the facilities for this research work.

REFERENCES

- [1] D. J. Q. J. Gao, "Enhancement of the Stress Corrosion Sensitivity of AA5083 by Heat Treatment," *Metall. Mater. Trans. A*, vol. 42 A, pp. 356-364, 2011.
- [2] H. H. Uhlig, "Corrosion and Corrosion Control," ed New York: Wiley, 1963.
- [3] Z. S. Toor, "Applications of Aluminum-matrix composites in Satellite: A Review," *Journal of Space Technology*, vol. 07, p. 1-6, 2017.
- [4] E. S. W. Dean and E. C. Rhea, "Atmospheric Corrosion of Metals," NACE, Ed., ed. Texas, 1980.
- [5] J. G. a. D. J. Quesnel, "Stress Corrosion Cracking of Sensitized AA5083 in NaCl Solution," in *NACE International CORROSION 2011 Conference*, Houston, Texas, 2011.
- [6] L. R. F. Allen J. Bard, *Electrochemical Methods: Fundamentals and Applications*.
- [7] S. U. Ishaq Ahmed, Zaigham Toor, Abdul Wadood, Akbar Niaz Butt, Syed Wilayat Hussain "Design, Fabrication and Beta testing of Four point Bend Immersion (FPBI) apparatus for the study of Stress Corrosion Cracking (SCC) " in *Student Research Paper Conference (SRPC) Institute of Space Technology (IST), Islamabad, Pakistan, 2015*, pp. 162-166.
- [8] A. Chennakesava Reddy, *Finite Element Analysis of Warm Deep Drawing Process for 2017T4 Aluminum Alloy: Parametric Significance Using Taguchi Technique* vol. 3, 2015.
- [9] A. Meyveci, İ. Karacan, U. Çalgülü, and H. Durmuş, "Pin-on-disc characterization of 2xxx and 6xxx aluminium alloys aged by precipitation age hardening," *Journal of Alloys and Compounds*, vol. 491, pp. 278-283, 2010/02/18/ 2010.

- [10] S. Bull. (1997). Al-Cu TTT Diagram. Available: <https://www.staff.ncl.ac.uk/s.j.bull/mmm211/aluminium/sld025.htm>
- [11] A. S. f. T. a. M. (ASTM), "Standard Practice for Preparation and Use of Bent-Beam Stress-Corrosion Test Specimens," in G-39, ed.
- [12] A. S. f. T. a. M. (ASTM), "Standard Reference Test Method for Making Potentiodynamic Anodic Polarization Measurements," in G-5, ed.
- [13] M. M. F.M. Queiroz , I. Costa, H.G. de Melo "Investigation of the corrosion behaviour of AA 2024-T3 in low concentrated chloride media," Corrosion Science, vol. 50, pp. 2646–2657, 2008.
- [14] A. E.-H. Hosni Ezuber , F. El-Shawesh, "A study on the corrosion behavior of aluminum alloys in seawater," Materials & Design, vol. 29, pp. 801-805, 2007.
- [15] J. R. Davis, Corrosion of Aluminum and Aluminum Alloys ASM International, 1999.
- [16] H. H. Uhlig, CORROSION AND CORROSION CONTROL An Introduction to Corrosion Science and Engineering fourth ed.: JOHN WILEY & SONS, INC, 1963.
- [17] D. X. L. T.F. Cui, P.A. Shi, J.J. Liu, Y.H. Yi and H.L. Zhou, "Effect of NaCl concentration, pH value and tensile stress on the galvanic corrosion behavior of 5050 aluminum alloy," Materials and Corrosion, vol. 67, 2016.
- [18] E. N. Pugh, "ON THE MECHANISM(S) OF STRESS-CORROSION CRACKING," Research Institute for Advanced Studies, Baltimore, Maryland, 1965. G. O. Young, "Synthetic structure of industrial plastics (Book style with paper title and editor)," in *Plastics*, 2nd ed. vol. 3, J. Peters, Ed. New York: McGraw-Hill, 1964, pp. 15–64.